Nonambipolar electron source

B. Longmier, S. Baalrud, and N. Hershkowitz
University of Wisconsin-Madison, Madison, Wisconsin 53706

(Received 15 September 2006; accepted 17 October 2006; published online 30 November 2006)

A radio frequency (rf) plasma-based electron source that does not rely on electron emission at a cathode surface has been constructed. All of the random electron flux incident on an exit aperture is extracted through an electron sheath resulting in total nonambipolar flow within the device when the ratio of the ion loss area to the electron loss area is approximately equal to the square root of the ratio of the ion mass to the electron mass, and the ion sheath potential drop at the chamber walls is much larger than T_e/e. The nonambipolar electron source (NES) has an axisymmetric magnetic field of 100 G at the extraction aperture that results in a uniform plasma potential across the aperture, allowing the extraction of all the incident electron flux without the use of grids. A prototype NES has produced 15 A of continuous electron current, using 15 SCCM (SCCM denotes cubic centimeter per minute at STP) Ar, 1200 W rf power at 13.56 MHz, and 6 times gas utilization. Alternatively 8 A of electron current can be produced, using 3 SCCM Ar at 1200 W rf and 20 times gas utilization. NES could replace hollow cathode electron sources in a wide variety of applications. © *2006 American Institute of Physics.* [DOI: 10.1063/1.2393164]

I. INTRODUCTION

Hollow cathodes are used in a variety of industrial applications[1–5] and are currently used as plasma and electron sources onboard spacecraft that employ ion thruster technology. Hollow cathodes have a finite lifetime, due largely to cathode deterioration, contamination, and barium diffusion rates.[6] This is usually not a problem for industrial applications; however, it can be a critical problem for spacecraft that use hollow cathode electron sources in a plasma generation stage or in a neutralization stage of an ion thruster, where long-duration continuous-thrust missions require an electron source with lifetimes in excess of the mission duration.[7] While using ion propulsion for longer-duration missions is beneficial because of fuel, mass, and time savings (as opposed to impulsive chemical rocket burns), the lifetime of some operating components for ion propulsion systems, such as the hollow cathode source, may be limited to three to four years,[7–9] thereby making longer continuous-thrust missions infeasible.

In gridded ion propulsion systems plasma is initially generated by energetic electrons from a hollow cathode and ions are extracted and accelerated by a series of differentially biased grids. The positive beam of ions is later neutralized with a stream of electrons that are introduced downstream of the ion acceleration grids by a second hollow cathode. Similarly, Hall thrusters use hollow cathodes as a source of plasma and as a source of electrons for neutralizing the accelerated ion beam. Traditionally, hollow cathode sources employing inserts with a refractory metal and a barium oxide-calcium oxide-aluminum oxide coating have been used as neutralizing sources on spacecraft because of their low work function, high electron current density, and relatively low power requirements.[9]

Radio frequency (rf) generated plasmas are attractive as electron sources for industrial plasma applications and electric propulsion devices because electron generation does not depend on cathode materials and they provide high ionization efficiency and long life operation. In this way, rf plasma sources provide an alternative approach to electron generation that does not consume electrode material while providing electrons, thereby allowing for high purity operation in industrial applications and for longer operational lifetimes in spacecraft thruster components. A variety of rf plasma sources exist including capacitive and inductive sources,[10,11] which can operate without magnetic fields, and both electron cyclotron resonance (ECR) and helicon sources, which require magnetic fields.[12] Helicon sources appear to be the best choice of rf plasma sources for use in high power/current ion propulsion because they have the highest ionization efficiency and can produce the highest plasma densities, up to 10^{13} cm^{-3} is common,[13] for a given rf power. The magnetic fields that are required for ECR and helicon plasma sources can be generated by electromagnets or permanent magnets. If insufficient rf power is available, helicon sources operate as inductive sources resulting in decreased plasma densities. At much lower rf powers, the plasma is capacitively coupled with even lower plasma densities.

ECR plasma sources have previously been used as a source of electrons for neutralizing gridded ion thrusters.[14,15] Microwave sources without applied magnetic fields have also been proposed for spacecraft neutralizer applications.[16,17] While efficient at plasma production, these devices to date have produced less than 2.5 A of electron beam current,[15–18] limiting their usefulness in higher current and higher thrust applications.

Experiments with the Phaedrus tandem mirror device[19] showed that the radial plasma potential interior to a magnetic flux tube can be controlled with an annular ring in the presence of an axial magnetic field. The nonintuitive result from that experiment is that the potential of the ring determines

the plasma potential for radii less than the radius of the ring. This result indicated the possibility of plasma potential control at a boundary.

Hollow cathode discharges are known as relatively efficient ion, electron, and plasma sources where dense plasma is formed interior to a hollow cylindrical cavity.[20] Ion sheaths form along the cavity walls and act to reflect and confine electrons in the bulk plasma. The electrostatic confinement of electrons leads to an efficient ionization of the working gas.[21] An electron sheath (a sheath where ion density can be neglected) forms across the exit aperture of hollow cathodes, acting to extract all or most incident electrons and to reflect all ions. In this way, there is a strong nonambipolar flow of electrons and ions with all of the electrons leaving the plasma through the aperture and all of the ions leaving the plasma at the cavity wall.

Here, we describe design problems and novel solutions for a high current/power rf plasma-based electron source that does not rely on grids for electron extraction or on physical cathode surfaces for electron production. The current proof of principle device has produced a plasma with densities from 10^{10} to 3×10^{12} cm^{-3} and is able to produce 15 A of continuous extracted electron current. The electron current is extracted through an electron sheath near a grounded ring located at the plasma source boundary, with a weak ($\sim$100 G) nonuniform axisymmetric magnetic field. Similarly, all of the ions that are lost within the device are extracted by a negatively biased conducting surface.

II. NONAMBIPOLAR FLOW IN ELECTRON SOURCES

In order to maintain quasineutrality during steady state operation, the amount of electron loss from the plasma must be balanced by an equal amount of ion loss.[22] Neglecting secondary emission from ion-wall collisions, which is small, electrons and ions are born at an equal rate within the rf discharge. Ultimately, plasma density and particle losses present the limiting factors for the total amount of electron current that can be extracted from the plasma for neutralizing an ion thruster.

A. Charged particle losses

The electron flux lost through the electron sheath is

$$J_e = \frac{n_e e \alpha_{e,e}}{4}\sqrt{\frac{8T_e}{\pi m_e}}, \tag{1}$$

where $\alpha_{e,e}$ is the transmission coefficient for electrons incident on an electron sheath. The transmission coefficient is defined as $\alpha_{j,k} \equiv \exp(-e\Delta\phi_k/T_e)$ for species j at sheath boundary k, $\alpha_{e,e}=1$ since all electrons incident on an electron sheath are lost, and $\alpha_{i,i}\approx 1/2$ because the Bohm presheath reduces the ion density at the ion sheath edge for retarding potential barriers. Similarly, the ion current to an ion sheath is the Bohm current

$$J_i = n_i e \alpha_{i,i}\sqrt{\frac{T_e}{m_i}}, \tag{2}$$

where $\alpha_{i,i}$ is the ion transmission coefficient incident on the ion sheath. Equating Eqs. (1) and (2), a global particle balance within nonambipolar electron source (NES) can be created for electrons and ions incident on both the electron sheath at the exit aperture and the ion sheath at the cylinder wall boundary.

$$\sqrt{\frac{m_i}{2\pi m_e}} = \frac{\alpha_{i,e}A_e + \alpha_{i,i}A_i}{\alpha_{e,e}A_e + \alpha_{e,i}A_i}, \tag{3}$$

where A_i is the ion loss area, A_e is the electron loss area, $\alpha_{i,e}$ is the ion transmission coefficient incident on the electron sheath, and $\alpha_{e,i}$ is the electron transmission coefficient incident on the ion sheath. Since $\Delta\phi \gg T_i/e$, $\alpha_{i,e}\rightarrow 0$, when $\Delta\phi_i \gg T_e/e$, $\alpha_{e,i}\rightarrow 0$ and all of the electrons will be extracted by the electron sheath. It is referred to as total nonambipolar flow when all electrons from a plasma are drawn out only by the electron sheath and all ions are drawn out only by the ion sheath. This total nonambipolar flow was previously performed using a dc filament produced plasma.[23] The plasma potential changes by at least $T_e/2$ from the bulk to the plasma-sheath boundary in order to provide acceleration in the Bohm presheath. The ratio of the ion density at the sheath edge to that of the bulk plasma is found from the Boltzmann relation, yielding $\alpha_{i,i}\approx 0.5$ for a weakly collisional plasma. Equation (3) then leads to

$$\frac{A_i}{A_e} \approx \sqrt{\frac{2m_i}{\pi m_e}}. \tag{4}$$

The limit to the existence of an electron sheath is provided by the condition that the ion loss current to area A_i be balanced by the electron loss current to area A_e. For large A_e, a pure electron sheath is no longer a viable solution, and a retarding potential dip will form to reduce the electron flux,[23] or the plasma potential becomes greater than the ring potential and an ion sheath forms at the anode.

In this experiment, ions are lost to the 5.6 cm diam graphite cylinder, with an ion loss area of 370 cm^2 and the electron loss region is restricted to a small 1.2 cm^2 aperture. This satisfies the condition that A_i must be larger than A_e by a factor of $\sqrt{2m_i/\pi m_e}\approx 230$ for Ar (410 for Xe) in order to maintain nonambipolar flow.

III. DESIGN ISSUES

Several design issues arose during the early stages of the rf plasma-based electron source development and are presented in this section; the design solutions for these issues are presented in Sec. IV.

A. Plasma potential fluctuations

In an effort to avoid dc filament and cathode surface material corrosion problems, rf generated plasmas were chosen, specifically inductively coupled plasmas and/or helicon plasmas. Capacitively generated plasmas were avoided because the plasma potential oscillates with a large amplitude on the time scale of the applied rf signal, which is usually less than the electron plasma frequency (except in microwave sources). For inductive and helicon sources, the amplitude of the plasma potential fluctuations is reduced, but may still be present because these plasma sources exhibit a portion of capacitive coupling and therefore a fluctuating plasma

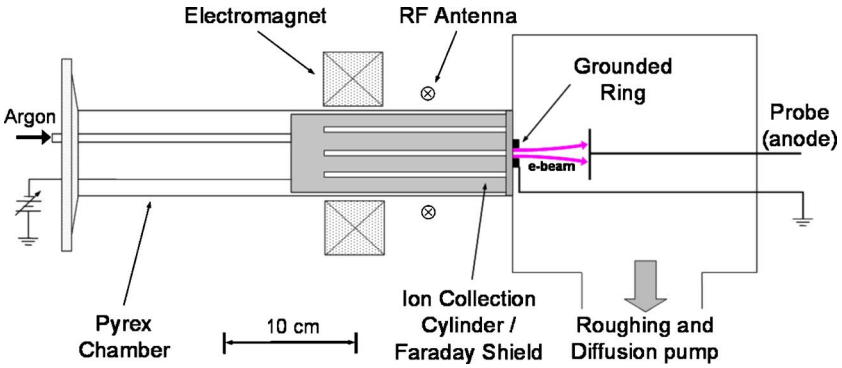

FIG. 1. (Color online) Schematic illustration of the plasma chamber containing the nonambipolar electron source (NES) with supporting vacuum hardware.

potential. In order to create an effective rf plasma-based electron source, the amplitude of the plasma potential fluctuations must be much less than the size of the voltage drop across the electron sheath that extracts the incident electron flux.

B. Ion and electron loss area

As outlined in Sec. II, the ion loss area must satisfy $A_i \geqslant A_e\sqrt{2m_i/\pi m_e}$ in order for all of the random electron flux to be extracted through an electron loss area A_e. For argon plasmas this means that the ion loss area must be at least 230 times larger than the electron loss area.

C. Electron and ion losses

In order for a griddles electron source to operate, some type of electrode or potential structure needs to exist to extract a population of electrons. The voltage drop across the resulting electron sheath must be larger than any plasma potential fluctuations that exist within the system.

If electrons are extracted through an orifice from a plasma, an equal number of ions must leave the plasma. This can be done with a conducting boundary that is biased more negatively than the plasma potential. In order to ensure that electrons are only lost at the orifice and not the negatively biased conducting boundary, the difference between the plasma potential and the boundary potential must satisfy $\Delta\phi_i \gg T_e/e$.

D. Gas utilization

In spacecraft applications it is desirable for the rf plasma-based electron source to use as little working gas as possible, thereby reducing the total mass of the fuel required and increasing the usable payload mass. The electron source should be designed such that the ratio of the extracted electron current to that of the neutral gas particle current (defined as the gas utilization) is maximized and should be equal to or greater than the gas utilization of hollow cathode devices.

IV. DESIGN SOLUTIONS

The hardware used in this experiment contains a nonambipolar electron source made up of an ion collection cylinder, electron extraction ring, rf antenna, Faraday shield, and an electromagnet; a vacuum chamber; a Langmuir probe/anode and an emissive probe; and argon feed gas. A schematic illustration of the plasma chamber containing NES and supporting vacuum hardware is shown in Fig. 1.

A. NES

A 5.6 cm inner diameter (i.d.), 7 cm outside diameter (o.d.), 21 cm long, hollow graphite cylinder is located coaxially within a Pyrex cylinder as the ion collection cylinder and can be biased from 0 to −100 V. This cylinder is a radial boundary for the plasma and acts as a location for the formation of an ion sheath that both collects ions and prevents electrons from leaking to the chamber walls. The ion collection cylinder has eight axial slots (1 mm wide), which allow the dB/dt fields into the plasma but limit the dE/dt fields,[24] effectively serving as a Faraday shield for the plasma within NES significantly reducing the amplitude of the plasma potential fluctuations. The electron extraction ring is an electrically grounded graphite ring with a 1.25 cm diam aperture that sits inside an insulating boron nitride disk. This grounded ring combined with the magnetic field creates an electron sheath, uniform across the area of the ring, limiting the ion flow, and giving a potential reference for the plasma somewhere near 0 to +5 V. The rf antenna is formed from a single turn of 0.25 in. water cooled copper tube and operates at power levels up to 1200 W at a rf of 13.56 MHz. The magnet coil geometry is discussed below and illustrated in Fig. 2.

B. Vacuum chamber

The components of the electron source are set within a 50 cm long 7.25 cm i.d. Pyrex tube. A diffusion pump and roughing pump create a base vacuum pressure of 5×10^{-7} Torr. With a standard operating Ar gas flow rate of 10 SCCM (SCCM denotes cubic centimeter per minute at STP), the chamber pressure external to the electron source is 6×10^{-4} Torr.

C. Diagnostic tools

A 0.1 mm diam tungsten emissive probe (not shown) is inserted from the right side of the chamber, see Fig. 1, and can be extended into the source side (left), and is used to determine the plasma potential along the entire axis within NES and in the plume region. A second bent emissive probe (not shown) is inserted from the source side (left) of NES and is swept in the axial direction and in the (r,θ) plane to measure radial variations in the plasma and floating poten-

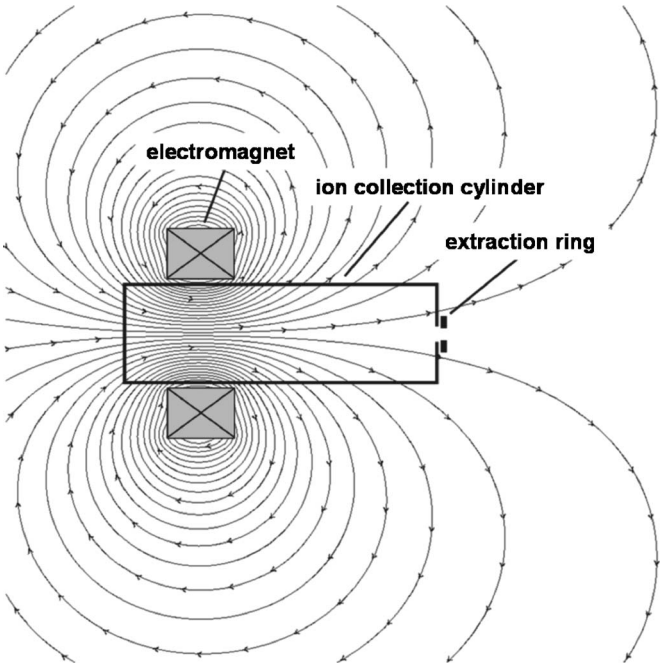

FIG. 2. Magnetic field lines for an axial cross section of the electromagnet coil. The ion collection cylinder and the electron extraction ring are superimposed into the field plot.

tials. The emissive probes are operated in the limit of zero emission, resulting in increased accuracy of plasma potential measurements.[25] A double probe is used for plasma density measurements. This type of probe is used because of its insensitivity to plasma potential fluctuations, as opposed to the time averaged *I-V* traces produced by typical Langmuir probes.

D. Feed gas

Argon feed gas is introduced into the chamber from a mass flow controller (not shown) and flows into the source region where a plasma is excited by the rf antenna.

E. Magnet geometry

An electromagnet coil generates an expanding dc magnetic field in the axial direction of the plasma chamber. Alternatively, a set of axially magnetized ferrite magnets is used to produce a similar steady state magnetic field with a fixed intensity and is located in the same position as the coil shown in Fig. 1. Either magnet arrangement produces a magnetic field in the region of the antenna and electron extraction ring. When present, the magnetic field ensures that the electrons follow the field lines that pass through the exit region of the electron extraction ring, and that fewer electrons are lost to the interior walls of the extraction ring. The presence of the magnetic field creates a uniform plasma potential across the surface of the extraction aperture, making uniform electron extraction possible. The magnetic field also acts to increase the plasma density, leading to an increased electron flux at the aperture and ultimately an increased electron current. Figure 2 shows the magnetic field lines for the single coil electromagnet.

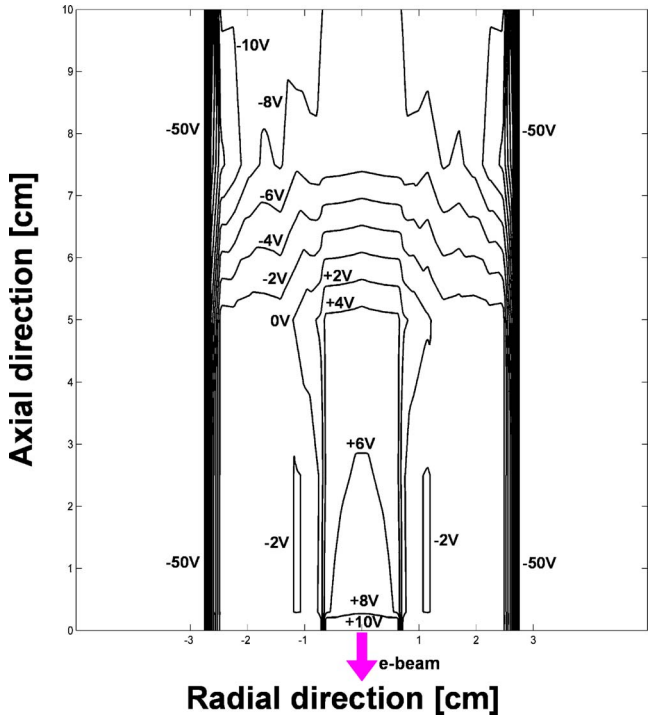

FIG. 3. (Color online) Equipotential contours of the plasma potential within the nonambipolar electron source. NES was operated using 600 W rf at 13.56 MHz, 10 SCCM Ar, −50 V bias on ion collection cylinder, and 100 G at the exit aperture.

V. EXPERIMENTAL RESULTS

A. Electron sheath behavior

Equipotential contours drawn from emissive probe data show that an electron sheath is present when electrons are being extracted, see Figs. 3 and 4. An emissive probe that was capable of sweeping out radial and axial positions within NES was used to determine the local plasma potential with an accuracy[25] of 0.2 V and a spatial resolution of 0.5 mm. Figures 3 and 4 show potential structures within NES and an electron sheath at the location of the extraction ring [lower middle of Fig. 3 and left side of Fig. 4(a)]. Inside of the grounded extraction ring, the plasma potential is held near the ring potential, as previously demonstrated by Severn and Hershkowitz.[19] The magnetic field strength not only plays an important role in increasing the plasma density but also allows for the formation of a uniform sheath across the exit aperture surface, as indicated by the relatively flat radial potential profile in Fig. 4(a) from a radius of 0 to 0.6 cm. In addition to the electron sheath at the boundary of the electron extraction ring, there is another potential structure that extends in the axial direction into the body of NES for the higher rf power level case, as seen in Fig. 4(b) as an axial cross section along the axis of the device. This structure follows the magnetic field lines within the chamber and is responsible for some of the electron extraction, although it is not associated with an increased A_e because the electron losses are axial. The ion sheath is located at the outer boundary of the dark overlapping contour lines in Fig. 3 and at a radius of 2.75 cm in Fig. 4(a).

A total nonambipolar condition is achieved by applying a sufficient negative bias to the ion collection cylinder such

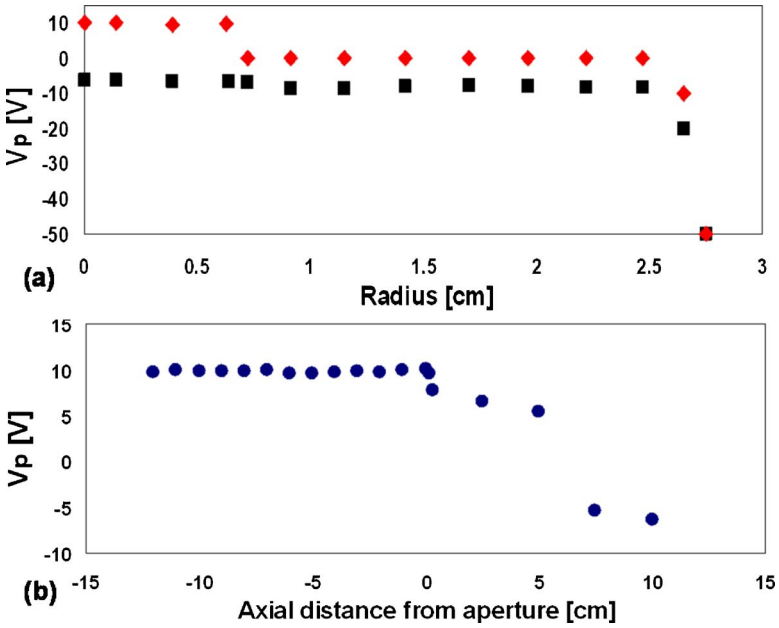

FIG. 4. (Color online) Transverse cross section of the plasma potential within NES at a 0 cm axial distance from the aperture (diamonds) and a 10 cm axial distance from the aperture (squares) (a), and axial cross section along the midplane (b). NES was operated using 600 W rf at 13.56 MHz, 10 SCCM Ar, −50 V bias on ion collection cylinder, and 100 G at the exit aperture.

that all electrons were reflected and the only remaining electron loss area was the exit aperture. This total nonambipolar flow occurs once a sufficiently negative bias is applied to the ion collection cylinder, in this case −35 V as seen in Fig. 5. The interior plasma potential changes from 0 to −10 V as the ion collection cylinder bias is varied from 0 to −50 V. Once total nonambipolar flow is established, the difference between the interior plasma potential and the anode potential remains fixed and no further current can be extracted. In this way, all of the electrons that are lost in the system are lost through the electron extraction aperture and all of the ions are lost to the ion extraction cylinder, thus allowing for the most efficient use of the plasma within NES. Similar plasma potential-anode potential locking has been observed in related dc sheath experiments.[21]

B. Neutral particle losses

When NES is operated with a plasma density of 3×10^{12} cm^{-3} at the extraction aperture, 15 A of electron current was extracted through a 1.2 cm^2 electron extraction aperture. If higher plasma densities are achieved, more current could be extracted or a smaller exit aperture could be used to achieve the same electron current extraction. If the exit aperture size is reduced, a lower gas flow rate will correspond to the same internal pressure, and hence the same internal plasma density. NES is essentially area limited in that the electron extraction current cannot exceed the random electron flux to the aperture or the ion extraction current that is collected by the ion loss area.

Ions are trapped within NES because of the large potential barrier that they see at the electron sheath ($\alpha_{i,e}\rightarrow0$) at the exit aperture, Fig. 4(b). Large recirculation rates of the ions occur within the system because ions are reflected at the aperture within NES, where only electrons and neutrals may leave the system through the aperture. NES recirculates ions and the electron current is not limited by the Bohm current at the extraction aperture, but rather it is only limited by the random electron flux at the extraction aperture. Hollow cathode electron sources exhibit a similar axial electron sheath structure at the extraction aperture.[26]

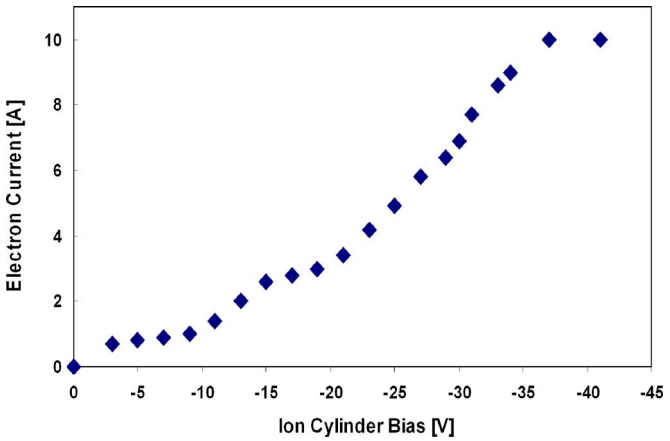

FIG. 5. (Color online) Electron current extracted to a grounded probe as a function of the ion collection cylinder bias. NES was operated using 1200 W rf at 13.56 MHz, 10 SCCM Ar, and 100 G at the exit aperture.

C. Gas utilization

For in-space electron source applications, it is beneficial to use a plasma production method that can create the largest ionization fraction possible so that neutral gas is not expelled before it can participate in electron production.

Gas utilization is defined as the ratio of electron current I_e that is extracted to the amount of neutral particle current I_p that flows out of the system, where 1 SCCM of neutral gas corresponds to a particle current of 0.072 A. In Fig. 6, the gas utilization within NES is graphed as a function of Ar flow rate for varying rf power levels. At a flow rate of 3 SCCM and 1200 W rf power, a 20 times gas utilization is achieved, which means that on average there are 20 electrons that exit the system for each neutral that exits the system. This is an intuitive result because as the applied rf power is increased from 300 to 1200 W for the same internal neutral

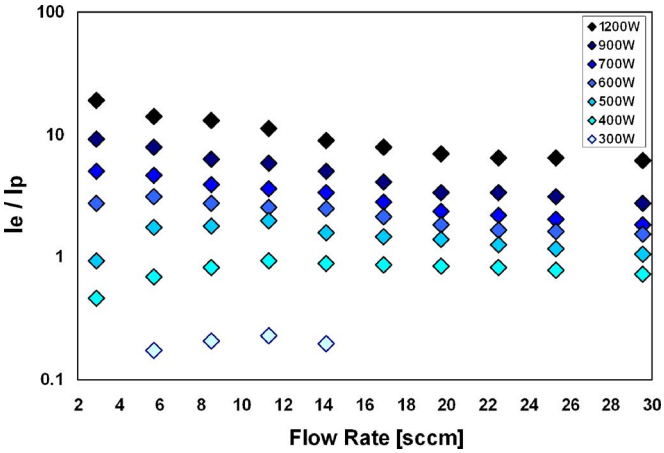

FIG. 6. (Color online) Extracted electron current divided by the neutral particle current as a function Ar flow rate for various rf power levels. 20 times gas utilization for 3 SCCM Ar at 1200 W rf at 13.56 MHz and 100 G at the exit aperture.

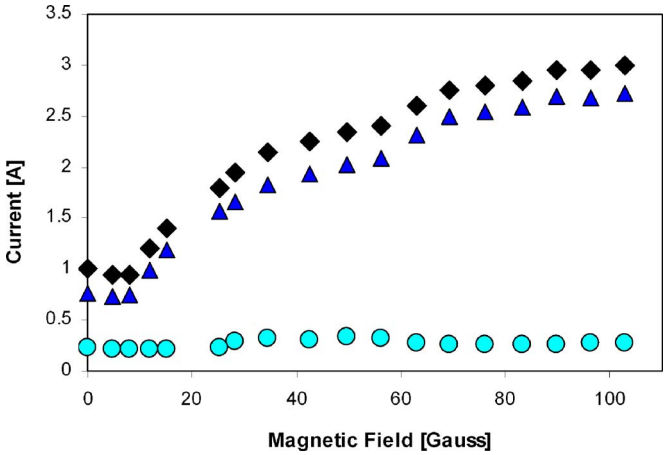

FIG. 7. (Color online) Ion current collected by the ion collection cylinder (diamonds), extracted electron current collected by a grounded probe (triangles), and electron current collected by the extraction ring (circles) as a function of magnetic field strength at the extraction aperture. NES was operated using 350 W rf at 13.56 MHz and 6 SCCM Ar.

pressures, the plasma density increases leading to an increased ionization fraction.

As the ionization fraction increases, the argon gas residence time increases because the average argon particle will spend more time as an ion. Ions are reflected at the extraction aperture within NES which leads to an improved gas utilization. As the applied rf power increases from 400 to 1200 W for the 3 SCCM case, the plasma density increases from 2×10^{11} to 2×10^{12} cm^{-3} and the ionization fraction increases from $\sim1:1000$ to $\sim1:100$, leading to a gas utilization increase from 0.5 to 20.

Figure 6 also indicates that there is a maximum gas utilization that occurs for any given applied rf power level. The maximum for 300, 400, and 500 W occurs at 11 and 6 SCCM for 600 W and the other maximum gas utilization points occur at 3 SCCM for higher power levels. Below 3 SCCM, the pressure within NES was too low to sustain a discharge for the 1.23 cm^2 aperture.

The gas utilization can also be improved by decreasing the extraction aperture size. This reduces the maximum amount of electron current that can be extracted, but it increases the minimum allowable gas flow rate to sustain a plasma discharge and increases the gas utilization for any given flow rate as seen in Fig. 6.

An ion born within NES is transported from the bulk plasma through the presheath and then to the ion sheath, accelerated to the Bohm velocity, where it contacts the cylinder wall and picks up an electron. The neutral gas particle is then free to travel back into the bulk of the NES chamber to be reionized. This reuse of neutrals is only possible because electrons and not ions, as is the case in ion thrusters, are being extracted through the NES aperture. If ions were extracted, as in an ion thruster, the ion outflow rate would never exceed the neutral inflow rate, but because NES is an electron source and is extracting electrons, the electron outflow rate can be many times the neutral gas inflow rate, where this ratio of electrons to neutrals depends on the plasma density, flow rate, and exit aperture size.

D. Magnetic field and rf power

The presence of a magnetic field allows for increased plasma densities by factors of 3–5 depending on the applied rf power. The applied axial magnetic field also allows for a large amount of electron current to be extracted from NES while reducing the fractional loss of electron current to the electron extraction aperture as seen in Fig. 7.

With zero applied magnetic field, the electron extraction current to an external anode is roughly 70% of the electron loss within the system, where the remaining 30% is lost to the electron extraction ring. The extraction ring is necessary in order to set the plasma potential at the boundary of NES, but if no magnetic field is present, then the ring can collect a large fraction of the electron current which leads to a reduced power efficiency of the electron source. As the applied magnetic field strength is increased from 0 to 110 G, the extracted ion and electron current increases as a result of increasing plasma density, while the current to the electron extraction ring remains relatively low. The electron current to the extraction ring remains relatively constant for increasing magnetic field strength. If the magnetic field is decreased to a point where the electrons have a gyroradius on the order of the aperture size, then the creation of a uniform plasma potential across the aperture is not possible. If the magnetic field is increased to a point much greater than 100 G, then the ion gyroradii become smaller than the dimensions of the ion collection cylinder, reducing the effective ion loss area within the electron source. The applied magnetic field strength of 100 G is large enough to confine the electrons radially with gyroradii much smaller than the loss aperture while letting the ions have gyroradii that are comparable to the chamber radius.

When the applied rf power is increased above 1000 W with an applied magnetic field of 100 G, a transition from an inductively coupled mode to a helicon mode occurs as seen in Fig. 8 by a large plasma density increase from double probe measurements. The sharp increase in plasma density over a narrow range of either magnetic field strength or rf

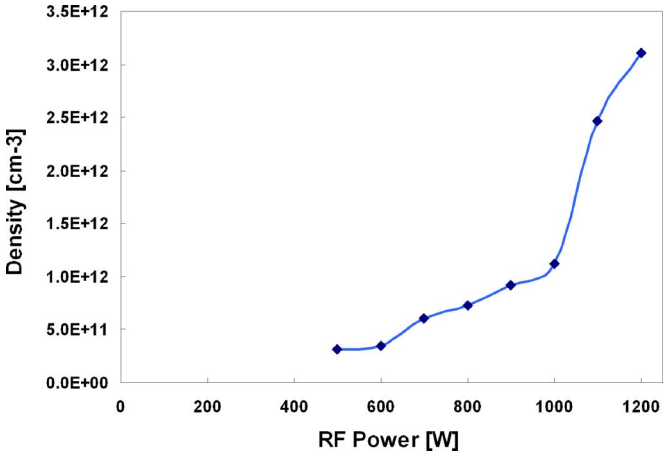

FIG. 8. (Color online) Plasma density at the antenna location, 8 cm from electron extraction aperture, as a function of the applied rf power at 13.56 MHz. NES was operated using 15 SCCM Ar and 100 G magnetic field.

power is associated with a mode change, in this case from an inductive mode to a helicon mode. A transition from capacitive mode to inductive mode is not observed because of the effectiveness of the Faraday shield at blocking the capacitive coupling to the plasma. Normally, inductive and helicon plasma sources are ignited through an initial capacitive mode coupling; however, because this mode is purposely blocked, a spark gap within the electron source is used to initiate the discharge.

The plasma density measurement of approximately 3×10^{12} cm^{-3}, achieved with 1200 W rf and 15 SCCM Ar, corresponds to an available electron flux density of $\sim$12.5 A/cm^2. The measured electron flux density of $\sim$12.2 A/cm^2 corresponds to 15 A of electron current extracted through a 1.23 cm^2 aperture. These two values of electron flux density, measured and calculated, agree to within the experimental uncertainty of the double probe measurements used to find the plasma density within the electron source.

VI. DISCUSSION

An electron sheath allows for the extraction of all the random electron flux through an exit aperture that is a factor of $\sqrt{2m_i/\pi m_e}$ smaller than the ion loss area located within the plasma source. The nonambipolar electron source (NES) has generated 15 A of electron current that could be used for the purposes of plasma processing or neutralization of a Hall or gridded ion thrusters. 15 A of extracted current was achieved using 15 SCCM Ar, 1200 W of rf power at 13.56 MHz, 100 G at the exit aperture, and a −40 V dc bias on the ion collection cylinder. The ion collection cylinder provided the necessary ion loss area while a smaller grounded ring was used to extract electrons through an electron sheath into the target region of the vacuum chamber. An axial expanding magnetic field created a uniform plasma potential across the exit aperture of NES which allowed for the extraction of all the incident electron flux. A unique feature of this proof of principle griddles electron source is the total nonambipolar extraction of electrons through an electron sheath, where all of the electrons in the system were extracted by the electron sheath at the exit aperture and all of the ions in the system were lost at the ion sheath at the chamber walls of NES.

The electron sheath at the exit aperture provides a large potential barrier which confines incident ions, but all neutrals and electrons that are incident on the exit aperture escape the system. The ratio of extracted electron current to neutral gas particle current was observed to be as high as 20, largely due to the fact that electron extraction is not accompanied by ion extraction at the aperture.

NES requires that $A_i/A_e \geqslant \sqrt{2m_i/\pi m_e}$ and $\Delta\phi_i \gg T_e/e$. The total amount of electron extraction current that NES can produce is ultimately limited by the electron loss area and the electron flux at the aperture. The fact that NES does not rely on material cathodes for the production of electrons should make it useful as an electron source for plasma processing applications and for continuous-thrust spacecraft missions using ion propulsion and may permit for missions that were previously unfeasible with conventional electron sources.

ACKNOWLEDGMENTS

The research described in this article was carried out at the University of Wisconsin-Madison, under an STTR grant with the National Aeronautics and Space Administration and was also supported in-part by the Wisconsin Space Grant Consortium to one of the authors (B.L.).

[1] H. Morgner, M. Neumann, S. Straach, and M. Krug, Surf. Coat. Technol. **108**, 513 (1998).
[2] B. Singh, O. R. Mesker, A. W. Levine, and Y. Aire, Appl. Phys. Lett. **52**, 1658 (2006).
[3] W. J. Chou, G. P. Yu, and J. H. Huang, Surf. Coat. Technol. **149**, 7 (2002).
[4] D. G. Williams, J. Vac. Sci. Technol. **11**, 374 (1974).
[5] A. Hellmich, T. Jung, A. Keilhorn, and M. Riszland, Surf. Coat. Technol. **98**, 1541 (1998).
[6] D. Goebel, I. Katz, J. Polk, I. G. Mikellides, K. K. Jameson, T. Liu, and R. Doughery, Proceedings of the AIAA Space 2004 Conference and Exposition, San Diego, CA, 28–30 September 2004, pp. 841–852.
[7] S. Oleson, Proceedings of the 40th Joint Propulsion Conference and Exhibit, Fort Lauderdale, FL, 11–14 July 2004, Paper No. AIAA-2004–3449.
[8] A. Sengupta, J. R. Brophy, and K. D. Goodfellow, Proceedings of the 39th Joint Propulsion Conference and Exhibit, Huntsville, AL, 20–23 July 2003, Paper No. AIAA 03-4558.
[9] T. Sarver-Verhey, Proceedings of the 26th International Electric Propulsion Conference, Kitakyushu, Japan, 17–21 October 1999, Paper No. IEPC-99–126.
[10] H. Kaufman and R. Robinson, U.S. Patent No. 4,954,751 (4 September 1990).
[11] R. G. Jahn, *Physics of Electric Propulsion* (Dover, New York, 2006), pp. 304–313.
[12] F. F. Chen, in *High Density Plasma Sources*, edited by O. A. Popov (Noyes, Park Ridge, NJ, 1995), Chap. 1, pp. 5–61; J. E. Stevens, *ibid.*, Chap. 7, pp. 312–355.
[13] J. Gilland, R. Breun, and N. Hershkowitz, Plasma Sources Sci. Technol. **7**, 416 (1998).
[14] H. Kuninaka, K. Nishiyama, Y. Shimizu, and K. Toki, Proceedings of the 40th Joint Propulsion Conference and Exhibit, Fomt. Lauderdale, FL, 11–14 July 2004, Paper No. AIAA-2004-3438.
[15] J. E. Foster, H. Kamhawi, T. Haag, C. Carpenter, and G. W. Williams, National Aeronautics and Space Administration Report No. NASA/TM-2006-214035, 2006.
[16] K. D. Diamant, Proceedings of the 41st Joint Propulsion Conference and Exhibit, Tucson, AZ, 10–13 July 2005, Paper No. AIAA-2005-3662.
[17] K. D. Diamant, Proceedings of the 42nd Joint Propulsion Conference and

Exhibit, Sacramento, CA, 9–12 July 2006 Paper No. AIAA-2006-5154.
[18] D. Korzec, A. Müller, and J. Engemann, Rev. Sci. Instrum. **71**, 800 (2000).
[19] G. D. Severn and N. Hershkowitz, Phys. Fluids B **4**, 3210 (1992).
[20] B. I. Moskalev, *Hollow Cathode Discharges* (Energiya, Moscow, 1969).
[21] E. M. Oks, A. Anders, and I. G. Brown, Rev. Sci. Instrum. **75**, 1030 (2004).
[22] F. F. Chen, Proceedings of the 37th Annual Meeting of the American Physical Society, Division of Plasma Physics, Louisville, KY, 6–10 November 1995, pp. 1783.
[23] S. Baalrud and N. Hershkowitz, Proceedings IEEE Conference Record-Abstracts, 33rd IEEE International Conference on Plasma Science, Traverse City, MI, 4–8 June 2006, p. 240.
[24] V. A. Godyak, R. B. Piejak, and B. M. Alexandrovich, Plasma Sources Sci. Technol. **4**, 332 (1995).
[25] N. Hershkowitz, in *Plasma Diagnostics*, edited by O. Auicello and D. L. Flamm (Academic, San Diego, 1989), Vol. 1, pp. 113–184.
[26] K. Jameson, D. Goebel, I. Mikellides, and R. Watkins, Proceedings of the 42nd Joint Propulsion Conference and Exhibit, Sacramento, CA, 9–12 July 2006, Paper No. AIAA-2006-4490.